Isomerization of Acetonitrile *N*-Methylide $[CH_3CNCH_2]^{\bullet+}$ and *N*-Methylketenimine $[CH_3NCCH_2]^{\bullet+}$ Radical Cations in the Gas Phase: Theoretical Study of the $[C_3,H_5,N]^{\bullet+}$ Potential Energy Surface

Jean-Yves Salpin and Minh Tho Nguyen*

University of Leuven, Department of Chemistry, Celestjinenlaan 200F, B-3001 Leuven, Belgium

Guy Bouchoux

Département de Chimie, Laboratoire des Mécanismes Réactionnels, UMR CNRS 7651, Ecole Polytechnique, 91128 Palaiseau Cedex, France

Pascal Gerbaux and Robert Flammang

Laboratoire de Chimie Organique, Université de Mons-Hainaut, Avenue Maistriau 19, B-7000 Mons, Belgium

Received: September 21, 1998; In Final Form: December 8, 1998

A theoretical study of the $[C_3,H_5,N]^{\bullet+}$ potential energy surface is presented. Ab initio molecular orbital calculations at the QCISD(T)/UMP2 level with the 6-31G(d,p) basis set show that acetonitrile *N*-methylide $[CH_3CNCH_2]^{\bullet+}$, $\mathbf{a}^{\bullet+}$, and *N*-methylketenimine $[CH_3NCCH_2]^{\bullet+}$, $\mathbf{b}^{\bullet+}$, are the most stable species among the 15 isomers considered, and a heat of formation of $\Delta_f H°_{298} = 970$ kJ/mol is proposed for both species. Detailed examination of the $[C_3,H_5,N]^{\bullet+}$ potential energy surface indicates that $\mathbf{a}^{\bullet+}$, $\mathbf{b}^{\bullet+}$, and related isomers are stable and distinct species in the gas phase, isolated by energy barriers as high as 300 kJ/mol. Their neutral equivalent, **a** and **b**, have also been studied, thus allowing their adiabatic ionization energies to be estimated: $IE_a(\mathbf{a}) = 7.1$ eV and $IE_a(\mathbf{b}) = 8.0$ eV. Finally, the theoretical study of $\mathbf{a}^{\bullet+}$ and $\mathbf{b}^{\bullet+}$ fragmentations provides an explanation for the similarity in their high-energy CID spectra by showing a possible isomerization of these species prior to dissociation.

Introduction

Ionized ketene[1] and ionized cyclobutanone[2] have been reported as efficient methylene transfer reagents. Under electron ionization, cyclobutanone gives rise to the distonic ion $[CH_2CH_2CH_2CO]^{\bullet+}$ and ionized ketene $[CH_2{=}C{=}O]^{\bullet+}$. Recently,[3] we reported that these ions react by methylene transfer reaction with acetonitrile and methyl isocyanide to generate acetonitrile *N*-methylide $[CH_3{-}C{\equiv}N{-}CH_2]^{\bullet+}$, $\mathbf{a}^{\bullet+}$, and *N*-methylketenimine $[CH_3{-}N{\equiv}C{-}CH_2]^{\bullet+}$, $\mathbf{b}^{\bullet+}$, radical cations, respectively. The distonic nature of both $\mathbf{a}^{\bullet+}$ and $\mathbf{b}^{\bullet+}$ has been clearly indicated by ion/molecule reactions with pyridine, whereas their different reactivity toward dimethyl disulfide (CH_3SSCH_3) revealed that $\mathbf{a}^{\bullet+}$ and $\mathbf{b}^{\bullet+}$ are stable and distinct structures in the gas phase. However, high-energy collision-induced dissociation (CID) experiments do not allow a clear-cut identification of $\mathbf{a}^{\bullet+}$ and $\mathbf{b}^{\bullet+}$ because of the similarity of recorded spectra, raising the question of interconversion between $\mathbf{a}^{\bullet+}$ and $\mathbf{b}^{\bullet+}$ under energetic conditions. To explain the experimental results, the present paper reports a theoretical study related to the $\mathbf{a}^{\bullet+} \rightarrow \mathbf{b}^{\bullet+}$ isomerization and the CID spectra main fragmentations.

Computational Details

Ab initio molecular orbital calculations have been carried out using the Gaussian-94 set of programs.[4] The different structures have first been optimized at the Hartree−Fock (HF) level with the dp-polarized 6-31G(d,p) basis set. Harmonic vibrational frequencies have been determined at this level in order to characterize stationary points as minima (equilibrium structures) or saddle points (transition structures) and scaled by a factor of 0.9 to estimate the zero-point energies. Geometrical parameters have subsequently been reoptimized by use of second-order Møller−Plesset perturbation theory. The MP2/6-31G(d,p) geometries have been finally utilized in single-point electronic energy calculations, in conjunction with the quadratic configuration interaction method. The unrestricted formalism (UHF, UMP2, UQCISD) has been employed for open-shell species. Throughout this paper total energies are expressed in hartree and relative energies in kJ/mol. Unless otherwise noted, the relative energies given thereafter are those obtained from UQCISD(T)/6-31G(d,p) total energies and corrected from zero-point vibrational energies (ZPE). Detailed geometries, total and relative energies at both UHF/6-31G(d,p) and UMP2/6-31G(d,p) levels, of all the structures mentioned in this paper, are available upon request to the authors.

Results and Discussion

1. $[C_3,H_5,N]$ and $[C_3,H_5,N]^{\bullet+}$ Isomers. To construct the $[C_3,H_5,N]^{\bullet+}$ potential energy surface, calculations for 15 cyclic and acyclic isomers have been performed. UQCISD(T)/6-31G(d,p) total and relative energies are summarized in Table 1, whereas optimized geometries are given by Figure 1 and Table 2. The structures $\mathbf{a}^{\bullet+}$, $\mathbf{b}^{\bullet+}$, $\mathbf{d}^{\bullet+}$, $\mathbf{e}^{\bullet+}$, $\mathbf{f}^{\bullet+}$, and $\mathbf{g}^{\bullet+}$ are distonic

* To whom correspondence should be addressed. E-mail: minh.nguyen@chem.kuleuven.ac.be.

10.1021/jp983796l CCC: $18.00
Published on Web 01/29/1999

TABLE 1: Calculated Total Energies (hartree) and Relative and Zero-Point Energies (kJ/mol) of the $[C_3,H_5,N]^{\bullet+}$, and $[C_3,H_5,N]$ Isomers Considered

structures	(u)QCISD(T)/6-31G(d,p)[a]	ZPE[b]	ΔE[c]
	Radical Cations		
a$^{\bullet+}$	−171.258 545	176	0
b$^{\bullet+}$	−171.259 785	178	−1
c$^{\bullet+}$	−171.249 304	179	+27
d$^{\bullet+}$	−171.241 222	175	+43
e$^{\bullet+}$	−171.257 047	178	+6
f$^{\bullet+}$	−171.228 680	179	+81
g$^{\bullet+}$	−171.240 002	177	+50
h$^{\bullet+}$	−171.174 14	182	+228
i$^{\bullet+}$	−171.167 541	184	+247
j$^{\bullet+}$	−171.204 605	181	+147
k$^{\bullet+}$	−171.223 261	179	+96
l$^{\bullet+}$	−171.088 268	176	+447
m$^{\bullet+}$	−171.221 612	178	+99
n$^{\bullet+}$	−171.212 632	189	+134
o$^{\bullet+}$	−171.210 736	181	+131
	Neutral Species		
a	−171.504 401	181	+235
b	−171.538 033	184	+149
h	−171.596 462	188	0
i	−171.559 559	187	+96
k	−171.558 901	199	+100
n	−171.540 967	191	+149

[a] Based on UMP2/6-31G(d,p) optimized geometries. [b] Zero-point energies based on UHF/6-31G(d,p) harmonic vibrational wavenumbers and scaled by 0.9. [c] Relatives energies including UQCISD(T)/6-31G(d,p) values and ZPE corrections.

ions in which charge and radical centers are formally separated, and the structures **c**$^{\bullet+}$, **h**$^{\bullet+}$, **i**$^{\bullet+}$, **k**$^{\bullet+}$, and **n**$^{\bullet+}$ correspond to the molecular ions of *N*-vinyl formaldimine, propionitrile, ethyl isocyanide, *E*-propenimine, and azetine, respectively. We have also considered two carbenic structures **l**$^{\bullet+}$ and **o**$^{\bullet+}$, the cumulenic ion **m**$^{\bullet+}$, and finally the cyclic ion **j**$^{\bullet+}$. All these ions are found to be local minima on the $[C_3,H_5,N]^{\bullet+}$ potential energy surface.

Regarding the relatives energies (Table 1), **a**$^{\bullet+}$ and **b**$^{\bullet+}$ have similar energies and are the two most stable forms among the various isomers considered. Both **a**$^{\bullet+}$ and **b**$^{\bullet+}$ possess a linear structure and a planar radical carbon center. Moreover, their bond lengths or distances between the terminal carbons are very similar. **h**$^{\bullet+}$ and **i**$^{\bullet+}$, the molecular ions of propionitrile and ethylisocyanide, are two reference structures for which accurate experimental thermochemical data are available. Use of experimental $\Delta_fH°_{298}(CH_3CH_2CN{=}\mathbf{h}) = 51$ kJ/mol[5] and IE(**h**) = 11.85 ± 0.02 eV [6] allows the determination of the value of the ion to be $\Delta_fH°_{298}(\mathbf{h}^{\bullet+}) = 1194 \pm 2$ kJ/mol. As for **i**$^{\bullet+}$, a heat of formation of 1222 ± 14 kJ/mol[7] has been deduced from IE(**i**) = 11.2 ± 0.1 eV[7,8] and an experimental value of $\Delta_fH°_{298}(CH_3CH_2NC{=}\mathbf{i}) = 141 \pm 4$ kJ/mol.[9] Note that the calculated difference in energy between **h**$^{\bullet+}$ and **i**$^{\bullet+}$ (19 kJ/mol) matches reasonably the difference in experimental heats of formation (28 kJ/mol). Results presented in Table 1 show that **h**$^{\bullet+}$ and **i**$^{\bullet+}$ are less stable than **a**$^{\bullet+}$ and **b**$^{\bullet+}$ by at least 228 kJ/mol. QCISD(T)/6-31G(d,p) calculations corrected for ZPE contributions, combined with the experimental $\Delta_fH°_{298}(\mathbf{h}^{\bullet+})$ and $\Delta_fH°_{298}(\mathbf{i}^{\bullet+})$, lead to an estimate of $\Delta_fH°_{298}(\mathbf{a}^{\bullet+}) \approx \Delta_fH°_{298}(\mathbf{b}^{\bullet+}) \approx 970$ kJ/mol, with a possible error of ±12 kJ/mol.

The observation of an important recovery signal during neutralization−reionization experiments[3] indicates that the

TABLE 2: UMP2/6-31G(d,p) Geometrical Parameters of the Different Structures

	bond lengths (in angström)					bond angles (in degrees)				
structures	b_1	b_2	b_3	b_4	b_5	a_1	a_2	a_3	a_4	a_5
				Radical Cations						
a$^{\bullet+}$	1.448	1.148	1.373							
b$^{\bullet+}$	1.439	1.143	1.411							
c$^{\bullet+}$	1.413	1.268	1.231			122.8	180.0			
d$^{\bullet+}$	1.480	1.369	1.139			119.1	180.0			
e$^{\bullet+}$	1.485	1.404	1.150			122.0	180.0			
f$^{\bullet+}$	1.487	1.481	1.158			109.8	180.0			
g$^{\bullet+}$	1.467	1.502	1.160			110.0	180.0			
h$^{\bullet+}$	1.535	1.410	1.207			116.2	180.0			
i$^{\bullet+}$	1.519	1.469	1.122			110.1	180.0			
j$^{\bullet+}$	1.462	1.431	1.390	1.329		140.0	60.3	63.5	56.2	
k$^{\bullet+}$	1.315	1.451	1.253			116.9	126.4			
l$^{\bullet+}$	1.449	1.287	1.420			136.8	122.3			
m$^{\bullet+}$	1.410	1.267	1.269			125.5	180.0			
n$^{\bullet+}$	1.478	1.568	1.534	1.248		79.6	87.9	88.4	104.4	
o$^{\bullet+}$	1.290	1.480	1.237			119.4	126.4			
				Neutral Species						
a	1.495	1.209	1.302			127.9	173.6			
b	1.465	1.233	1.320			121.2	175.6			
h	1.530	1.466	1.181			112.1	180.0			
i	1.522	1.429	1.191			111.1	180.0			
k	1.342	1.461	1.288			122.2	120.3			
n	1.501	1.552	1.499	1.302		89.7	80.6	100.3	89.3	
				Transition Structures						
TS **a**$^{\bullet+}$/**b**$^{\bullet+}$	1.407	1.195	1.516	1.441	1.431	78.0	142.4	97.3	94.0	128.3
TS **a**$^{\bullet+}$/**c**$^{\bullet+}$	1.282	1.237	1.373	1.427	1.231	129.7	128.3	66.2	52.1	
TS **a**$^{\bullet+}$/**d**$^{\bullet+}$	1.476	1.313	1.306	1.338	1.301	132.3	80.9	97.5	80.1	99.0
TS **a**$^{\bullet+}$/**m**$^{\bullet+}$ [a]	1.359	1.247	1.486	1.496	1.304	148.3	106.9	68.0	103.4	81.6
TS **b**$^{\bullet+}$/**c**$^{\bullet+}$	1.378	1.303	1.404	1.537	1.191	133.7	78.6	90.6	76.8	114.0
TS **b**$^{\bullet+}$/**m**$^{\bullet+}$	1.283	1.253	1.394	1.348	1.232	175.5	138.9	61.4	53.4	
TS **c**$^{\bullet+}$/**d**$^{\bullet+}$	1.266	1.340	1.459	1.397	1.352	108.4	112.5	88.2	118.1	102.8
TS **c**$^{\bullet+}$/**m**$^{\bullet+}$	1.254	1.394	1.266	1.368	1.260	149.3	148.6	54.3	61.8	
TS **c**$^{\bullet+}$/**o**$^{\bullet+}$ [a]	1.342	1.406	1.221	1.314	1.243	120.4	156.9	64.5	58.6	
TS **d**$^{\bullet+}$/**f**$^{\bullet+}$	1.469	1.384	1.142	1.251	1.325	118.9	177.6	57.6	52.9	
TS **d**$^{\bullet+}$/**o**$^{\bullet+}$ [a]	1.490	1.339	1.259	1.365	1.450	98.7	148.1	76.8	99.5	85.0
TS **f**$^{\bullet+}$/**o**$^{\bullet+}$	1.367	1.427	1.222	1.405	1.331	116.0	144.7	56.1	62.8	

[a] UHF/6-31G(d,p) optimized geometries.

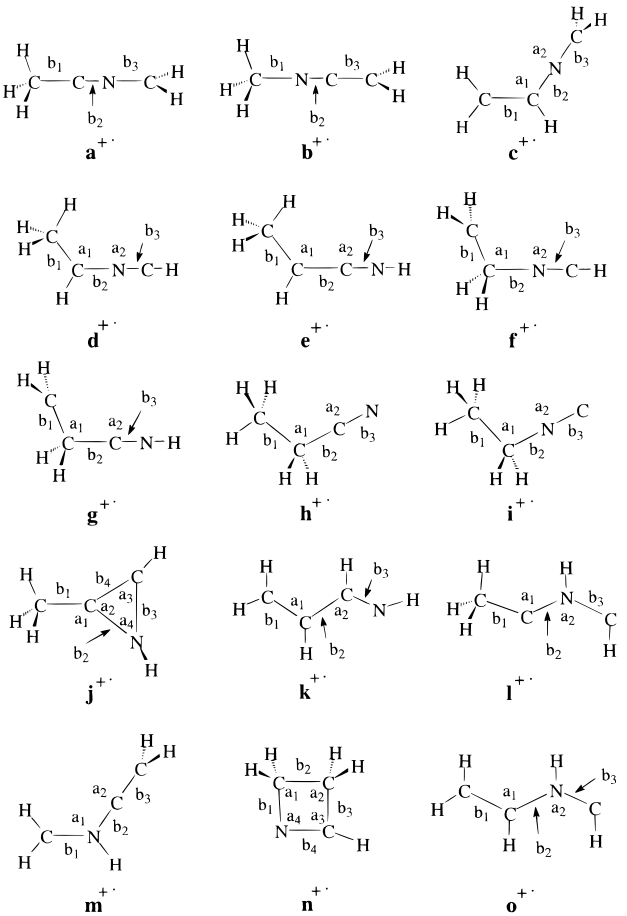

Figure 1. Optimized geometries of the $[C_3,H_5,N]^{\bullet+}$ isomers at the UMP2/6-31G(d,p) level. See Table 2 for bond lengths (b_x) and bond angles (a_x).

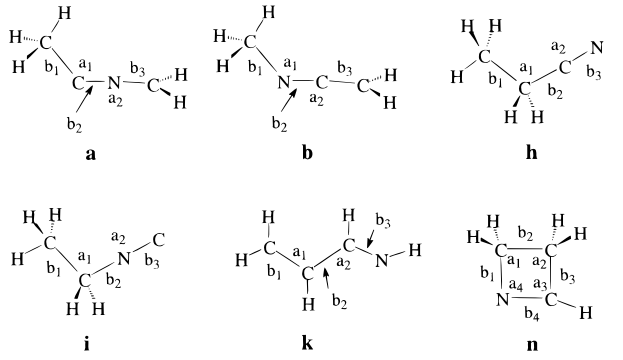

Figure 2. Optimized geometries of $[C_3H_5N]$ isomers at the UMP2/6-31G(d,p) level. See Table 2 for bond lengths (b_x) and bond angles (a_x).

neutral counterparts $CH_3-C-N=CH_2$, **a**, and $CH_3-N=C=CH_2$, **b**, are stable species in the gas phase. To probe their stability, we have performed ab initio calculations for six neutral species including **a** and **b**, together with propionitrile (**h**), ethyl isocyanide (**i**), *E*-propenimine (**k**), and azetine (**n**) (see Figure 2 and Table 2). Results are also summarized in Table 1. Both molecules **a** and **b** correspond to minima on the $[C_3,H_5,N]$ potential energy surface, thus confirming the experimental observations, but are the least stable isomers studied. Moreover, calculation predicts that **b** is more stable than **a** by 86 kJ/mol. We may also note that for **h** and **i**, the calculated relative energy of 96 kJ/mol is in good agreement with the difference in experimental heat of formation (90 kJ/mol). Combination of relative energies and the known heats of formation $\Delta_fH°_{298}$(**h**) and $\Delta_fH°_{298}$(**i**) leads to $\Delta_fH°_{298}$(**a**) ≈ 282 kJ/mol and $\Delta_fH°_{298}$(**b**) ≈ 197 kJ/mol.

Given the definition of ionization energy, $IE_a = \Delta_fH°(ion^{\bullet+}) - \Delta_fH°(neutral)$, we can deduce from the estimated heats of formation of **a**, **b**, $\mathbf{a}^{\bullet+}$, and $\mathbf{b}^{\bullet+}$ the adiabatic ionization energies of 7.1 and 8.0 eV for **a** and **b**, respectively. These values provide some insight into the difference in reactivity of $\mathbf{a}^{\bullet+}$ and $\mathbf{b}^{\bullet+}$ toward dimethyl disulfide (DMDS).[3] Ion $\mathbf{a}^{\bullet+}$ reacts with DMDS, mainly by $CH_3S^{\bullet}$ abstraction (92%), charge exchange being a minor process (8%). The opposite reactivity is observed with ion $\mathbf{b}^{\bullet+}$, where charge transfer is predominant (93%) versus 7% for $CH_3S^{\bullet}$ abstraction:

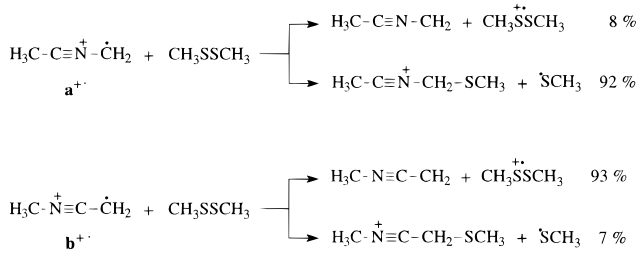

Since exothermic charge-transfer reactions usually occur at collision rate,[10] the charge-transfer reaction is very probably endothermic with $\mathbf{a}^{\bullet+}$ but exothermic with $\mathbf{b}^{\bullet+}$. An ionization energy of 8.0 ± 0.2 eV for **b** has been recently deduced from bracketing experiments by Leeck et al.[11] Therefore, the comparison of this value with the calculated ionization energies of **a** and **b** is in agreement with the observed reactivity. Finally, observation of a charge-transfer reaction with ion $\mathbf{a}^{\bullet+}$ may be due to the fact that endothermic reactions may occur in the rf-only quadrupole collision cell of the Mons Micromass Autospec-6F mass spectrometer,[12] owing to the absence of thermalization of ions prior to reaction.

The ions $\mathbf{d}^{\bullet+}$ and $\mathbf{e}^{\bullet+}$ are the tautomeric imine forms of $\mathbf{i}^{\bullet+}$ and $\mathbf{h}^{\bullet+}$, respectively. According to Table 1, $\mathbf{d}^{\bullet+}$ and more particularly $\mathbf{e}^{\bullet+}$ are very stable species. UQCISD(T)/6-31G(d,p) + ZPE relative energies predict on one hand that $\Delta_fH°_{298}(\mathbf{i}^{\bullet+})$ is 204 kJ/mol higher than $\Delta_fH°_{298}(\mathbf{d}^{\bullet+})$ and that $\mathbf{e}^{\bullet+}$ is about 222 kJ/mol more stable than ionized propionitrile. These results are in agreement with what has been observed for the $[CH_3C{\equiv}N]^{\bullet+}/[CH_2C{=}NH]^{\bullet+}$ and $[CH_3N{\equiv}C]^{\bullet+}/[CH_2N{=}CH]^{\bullet+}$ tautomerism[8] and for various keto−enol isomers. In fact, the enol radical cations are usually more stable than the corresponding keto forms.[13] Finally, it is worth mentioning that according to CID experiments,[8] $\mathbf{e}^{\bullet+}$ ions are stable species in the gas phase.

The cumulenic structure $\mathbf{l}^{\bullet+}$ has been proposed by Rusli and al.[14] as an intermediate in the loss of $CH^{\bullet}$ radical from $\mathbf{a}^{\bullet+}$ ions generated by reaction of ionized cyclopropane with acetonitrile. However, *m*/*z* 42 ions have not been observed in our experiments. Calculations show that $\mathbf{l}^{\bullet+}$ is indeed a minima but is by far the least stable $[C_3,H_5,N]^{\bullet+}$ isomer. Moreover, attempts to locate a transition structure between $\mathbf{l}^{\bullet+}$ and $\mathbf{j}^{\bullet+}$ failed. It revealed a continuous increase of energy from $\mathbf{j}^{\bullet+}$ to $\mathbf{l}^{\bullet+}$.

Calculated relative energies indicate that the molecular ion of the *E*-propenimine, $\mathbf{k}^{\bullet+}$, is 132 and 151 kJ/mol more stable than $\mathbf{h}^{\bullet+}$ and $\mathbf{i}^{\bullet+}$, respectively, thus leading to an estimated $\Delta_fH°_{298}(\mathbf{k}^{\bullet+})$ of 1067 kJ/mol. Combination of the latter value with the experimental ionization energy of *E*-propenimine **k** (9.65 eV[15]) leads to $\Delta_fH°_{298}(\mathbf{k})$ = 136 kJ/mol. This estimate is in a good agreement with the experimental heat of formation of **k** (125 ± 10 kJ/mol) deduced from its proton affinity[16] and with the calculated value at the MP2/6-311++G(d,p)//MP2/6-31G(d) level (128 kJ/mol[16]). Note that a direct use of $[C_3,H_5,N]$

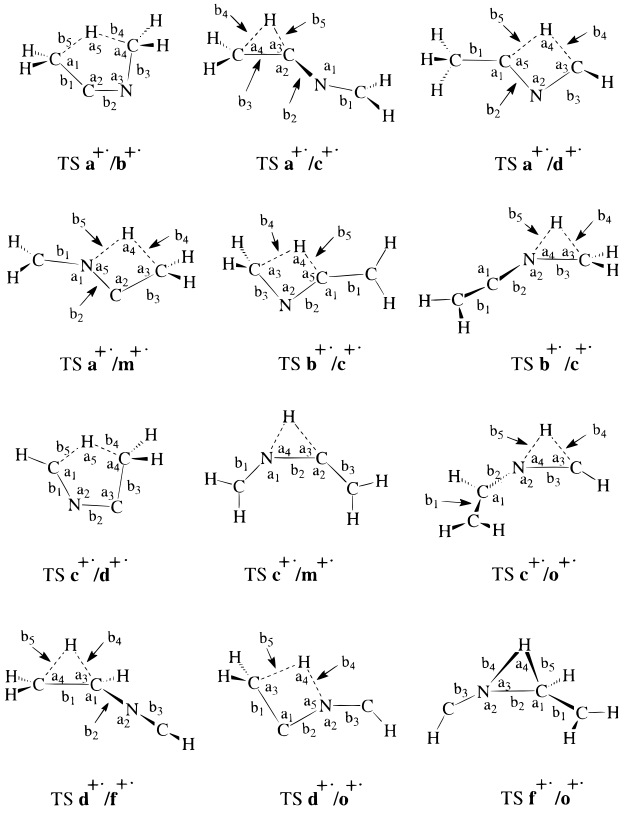

Figure 3. Optimized geometries of the transition-state structures involved in the isomerization of $[C_3,H_5,N]^{\bullet+}$ species. See Table 2 for bond lengths (b_x) and bond angles (a_x).

relative energies from this work leads to a slightly different estimate (151 kJ/mol).

Finally, we have also studied both neutral and ionized azetine (**n** and $\mathbf{n}^{\bullet+}$). Calculated relative energies indicate that $\mathbf{n}^{\bullet+}$ is 94 and 113 kJ/mol more stable than $\mathbf{h}^{\bullet+}$ and $\mathbf{i}^{\bullet+}$, respectively, matching well the differences of experimental heats of formation (86 and 114 kJ/mol, respectively[7]). By taking **h** and **i** as references, we deduce $\Delta_f H°_{298}(\mathbf{n}) = 197$ kJ/mol, which is 14 kJ/mol below this estimated value mentioned in ref 7.

2. Unimolecular Chemistry of $\mathbf{a}^{\bullet+}$ and $\mathbf{b}^{\bullet+}$. *A. $a^{\bullet+} \rightarrow b^{\bullet+}$ Isomerization.* Recently[3], we have reported that high-energy CID spectra of $\mathbf{a}^{\bullet+}$ and $\mathbf{b}^{\bullet+}$ are very similar and therefore not conclusive concerning the connectivity of the atoms. This similarity raises the question of a possible interconversion of $\mathbf{a}^{\bullet+}$ and $\mathbf{b}^{\bullet+}$ prior to dissociation. The $\mathbf{a}^{\bullet+} \rightarrow \mathbf{b}^{\bullet+}$ isomerization is studied in the present work by considering various reversible 1,*n*-hydrogen shifts ($n = 2$, 3, 4) between several $[C_3,H_5,N]^{\bullet+}$ species described in the first section. UMP2/6-31G(d,p) optimized geometries of the transition structures are presented in Figure 3. The corresponding geometrical parameters are given in Table 2. Relative energies by reference to $\mathbf{a}^{\bullet+}$, at the UQCISD(T)/6-31G(d,p) + ZPE level, are listed in Table 3. The energetic results are illustrated by Figure 4. Note that for TS $\mathbf{a}^{\bullet+}/\mathbf{m}^{\bullet+}$, TS $\mathbf{c}^{\bullet+}/\mathbf{o}^{\bullet+}$, and TS $\mathbf{d}^{\bullet+}/\mathbf{o}^{\bullet+}$, the UQCISD(T)/6-31G(d,p) energies correspond to a single-point energy calculation using the UHF/6-31G(d,p) geometries, since intensive attempts of optimization involving electron correlation for these three transition-state structures failed.

Starting from $\mathbf{a}^{\bullet+}$, there are several possible migrations, namely, a 1,4-H shift (the direct isomerization $\mathbf{a}^{\bullet+} \rightarrow \mathbf{b}^{\bullet+}$), two 1,2-H shifts ($\mathbf{a}^{\bullet+} \rightarrow \mathbf{c}^{\bullet+}$ or $\mathbf{a}^{\bullet+} \rightarrow \mathbf{l}^{\bullet+}$), and two 1,3-H shifts ($\mathbf{a}^{\bullet+} \rightarrow \mathbf{m}^{\bullet+}$ or $\mathbf{a}^{\bullet+} \rightarrow \mathbf{d}^{\bullet+}$). The calculations indicate that the one-step $\mathbf{a}^{\bullet+} \rightarrow \mathbf{b}^{\bullet+}$ isomerization, associated with an energy barrier of 345 kJ/mol, is not the most favorable process. The easiest process leads to the $\mathbf{c}^{\bullet+}$ structure, via a 1,2-H migration ($\mathbf{a}^{\bullet+}$ and $\mathbf{c}^{\bullet+}$ being connected by a transition state lying 252 kJ/mol above $\mathbf{a}^{\bullet+}$). Optimization of TS $\mathbf{a}^{\bullet+}/\mathbf{l}^{\bullet+}$ failed. Finally, the two 1,3-H shifts, leading to $\mathbf{d}^{\bullet+}$ and $\mathbf{m}^{\bullet+}$ ions, require more activation energy than the $\mathbf{a}^{\bullet+} \rightarrow \mathbf{c}^{\bullet+}$ interconversion, the associated transition structures being 122 and 230 kJ/mol above TS $\mathbf{a}^{\bullet+}/\mathbf{c}^{\bullet+}$, respectively.

The ions $\mathbf{c}^{\bullet+}$ may also evolve according to different H displacements. The 1,4-H shift leading $\mathbf{c}^{\bullet+}$ to $\mathbf{d}^{\bullet+}$ is associated with a transition structure located at 243 kJ/mol above $\mathbf{c}^{\bullet+}$. This channel is, however, more favorable than the stepwise mechanism $\mathbf{c}^{\bullet+} \rightarrow \mathbf{o}^{\bullet+} \rightarrow \mathbf{f}^{\bullet+} \rightarrow \mathbf{d}^{\bullet+}$ involving three successive 1,2-H shifts. In examining Table 3 and Figure 4, we can see that the $\mathbf{c}^{\bullet+} \rightarrow \mathbf{b}^{\bullet+}$ process is privileged compared to the two-step $\mathbf{c}^{\bullet+} \rightarrow \mathbf{m}^{\bullet+} \rightarrow \mathbf{b}^{\bullet+}$. Therefore, the best pathway for the $\mathbf{a}^{\bullet+}/\mathbf{b}^{\bullet+}$ interconversion is the two-step $\mathbf{a}^{\bullet+} \rightarrow \mathbf{c}^{\bullet+} \rightarrow \mathbf{b}^{\bullet+}$ process, requiring $\mathbf{a}^{\bullet+}$ and $\mathbf{b}^{\bullet+}$ ions to have about 300 kJ/mol of internal energy. These results clearly indicate that the different $[C_3,H_5,N]^{\bullet+}$ structures are separated from each other by high-energy barriers and therefore lie in very deep energy wells. Consequently, the different $[C_3,H_5,N]^{\bullet+}$ ions involved in these isomerization processes appear to be a stable and distinct species in the gas phase. Thus, $\mathbf{a}^{\bullet+}$ and $\mathbf{b}^{\bullet+}$ ions with no internal energy (that means relaxed to thermal energy) are not expected to isomerize. This result is in excellent agreement with the difference in reactivity of $\mathbf{a}^{\bullet+}$ and $\mathbf{b}^{\bullet+}$ toward dimethyl disulfide (DMDS), since these experiments involved a deceleration of reacting ions

TABLE 3: Calculated Total Energies (hartree) and Relative and Zero-Point Energies (kJ/mol) of the Different Transition Structures Involved in the Isomerization Processes

structures	corresponding TS number	(u)QCISD(T)/6-31G(d,p)[a]	ZPE[c]	ΔE[d]
TS $\mathbf{a}^{\bullet+}/\mathbf{b}^{\bullet+}$ (1,4-H shift)	TS1	−171.125 573	169	+345
TS $\mathbf{a}^{\bullet+}/\mathbf{c}^{\bullet+}$ (1,2-H shift)	TS2	−171.161 338	173	+252
TS $\mathbf{a}^{\bullet+}/\mathbf{d}^{\bullet+}$ (1,3 H shift)	TS3	−171.112 347	166	+374
TS $\mathbf{a}^{\bullet+}/\mathbf{m}^{\bullet+}$ (1,3-H shift)	TS4	−171.063 683[b]	160	+482
TS $\mathbf{b}^{\bullet+}/\mathbf{c}^{\bullet+}$ (1,3-H shift)	TS5	−171.142 896	172	+300
TS $\mathbf{b}^{\bullet+}/\mathbf{m}^{\bullet+}$ (1,2-H shift)	TS6	−171.130 693	161	+321
TS $\mathbf{c}^{\bullet+}/\mathbf{d}^{\bullet+}$ (1,4-H shift)	TS7	−171.152 096	168	+270
TS $\mathbf{c}^{\bullet+}/\mathbf{m}^{\bullet+}$ (1,2-H shift)	TS8	−171.115 469	161	+361
TS $\mathbf{c}^{\bullet+}/\mathbf{o}^{\bullet+}$ (1,2-H shift)	TS9	−171.128 593[b]	163	+328
TS $\mathbf{d}^{\bullet+}/\mathbf{f}^{\bullet+}$ (1,2-H shift)	TS10	−171.163 012	165	+240
TS $\mathbf{d}^{\bullet+}/\mathbf{o}^{\bullet+}$ (1,3-H shift)	TS11	−171.076 797[b]	155	+456
TS $\mathbf{f}^{\bullet+}/\mathbf{o}^{\bullet+}$ (1,2-H shift)	TS12	−171.102 292	164	+398

[a] Based on UMP2/6-31G(d,p) optimized geometries. [b] Based on UHF/6-31G(d,p) optimized geometries. [c] Zero-point energies based on UHF/6-31G(d,p) harmonic vibrational wavenumbers and scaled by 0.9. [d] Relatives energies ($\mathbf{a}^{\bullet+}$ being the reference) including UQCISD(T)/6-31G(d,p) values and ZPE corrections.

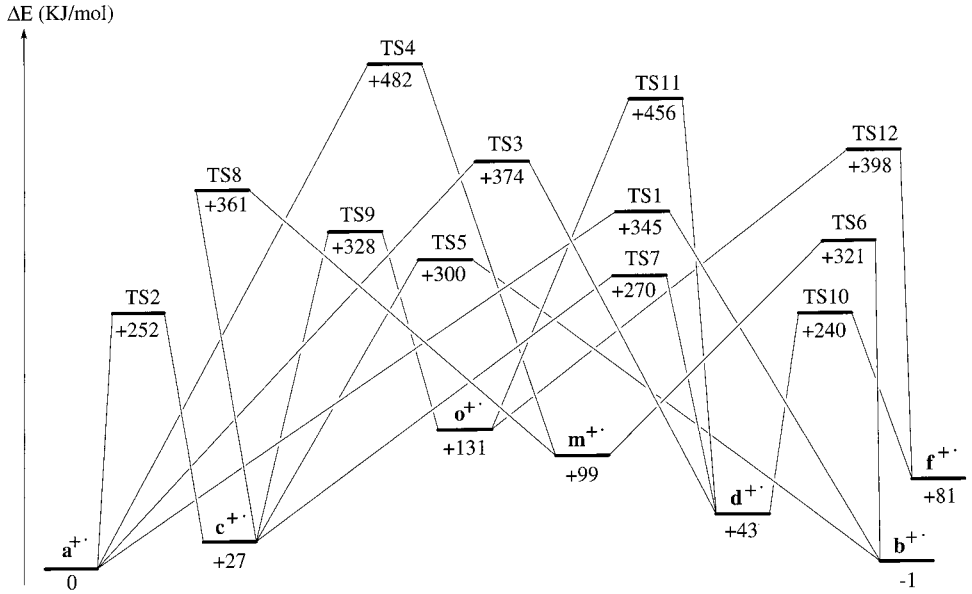

Figure 4. Stationary points on the potential energy surface related to the $\mathbf{a}^{\bullet+} \rightarrow \mathbf{b}^{\bullet+}$ isomerization.

TABLE 4: Calculated Total Energies (hartree)) and Relative and Zero-Point Energies (kJ/mol) of Fragments Corresponding to Formation of *m/z* 14, *m/z* 15, *m/z* 40, *m/z* 41, and *m/z* 54 Ions

structures	corresponding fragment number	(u)QCISD(T)/6-31G(d,p)[a]	ZPE[b]	ΔE[c]
		Formation of *m/z* 54		
$H^{\bullet} + CH_3CNCH^+$	**1 + 2**	−171.063 502	145	+481
$H^{\bullet} + CH_2CNCH_2^+$	**1 + 3**	−171.151 602	155	+260
$H^{\bullet} + CH_3NCCH^+$	**1 + 4**	−171.050 986	153	+522
$H^{\bullet} + CH_2CHNCH^+$	**1 + 5**	−171.166 797	157	+222
$H^{\bullet} + CH_2CHCNH^+$	**1 + 6**	−171.182 372	157	+181
TS $\mathbf{c}^{\bullet+}$**/1 + 5**	**TS13**	−171.154 296	154	+252
TS $\mathbf{d}^{\bullet+}$**/1 + 5**	**TS14**	−171.157 952	156	+244
TS $\mathbf{f}^{\bullet+}$**/1 + 5**	**TS15**	−171.151 040	157	+263
TS $\mathbf{o}^{\bullet+}$**/1 + 5**	**TS16**	−171.132 470	152	+307
		Formation of *m/z* 14		
$CH_2^{\bullet+} + CH_3CN$	**7 + 8**	−171.068 094	156	+480
$CH_2^{\bullet+} + CH_3NC$	**7 + 9**	−171.027 903	156	+586
$CH_2^{\bullet+} + CH_2CNH$	**7 + 10**	−171.016 042	153	+614
$CH_2^{\bullet+} + CH_2NCH$	**7 + 11**	−170.969 525	150	+733
$CH_2^{\bullet+} + CH_2CHN$	**7 + 12**	−170.959 253	147	+757
		Formation of *m/z* 15		
$CH_3^+ + CH_2NC^{\cdot}$	**13 + 14**	−171.068 707	154	+476
$CH_3^+ + CH_2CN^{\cdot}$	**13 + 15**	−171.106 402	155	+378
		Formation of *m/z* 40		
$^{\cdot}CH_3 + {}^+CH_2NC$	**16 + 17**	−171.089 794	+154	+421
$^{\cdot}CH_3 + {}^+CH_2CN$	**16 + 18**	−171.094 768	+153	+407
$^{\cdot}CH_3 + HCNCH^+$	**16 + 19**	−171.043 935	+147	+534
		Formation of *m/z* 41		
$CH_2 + CH_3CN^{\bullet+}$	**20 + 21**	−170.969 321	+153	+736
$CH_2 + CH_3NC^{\bullet+}$	**20 + 22**	−170.998 877	+156	+662
$CH_2 + CH_2CNH^{\bullet+}$	**20 + 23**	−171.081 464	+148	+437
$CH_2 + CH_2NCH^{\bullet+}$	**20 + 24**	−171.056 025	+147	+479

[a] Based on UMP2/6-31G(d,p) optimized geometries. [b] Zero-point energies based on UHF/6-31G(d,p) harmonic vibrational wavenumbers and scaled by 0.9. [c] Relatives energies including UQCISD(T)/6-31G(d,p) values and ZPE corrections, by reference to $\mathbf{a}^{\bullet+}$.

preceding the reaction with DMDS in the rf-only quadrupole collision cell.[3]

B. Study of High-Energy CID Spectra of $\boldsymbol{a}^{\bullet+}$ *and* $\boldsymbol{b}^{\bullet+}$. As mentioned earlier, the high-energy CID spectra of $\mathbf{a}^{\bullet+}$ and $\mathbf{b}^{\bullet+}$ are very similar and dominated by signals at m/z 54 and 28, but significant peaks also appear at m/z 14, 15, 27, 40, and 41. To understand such a similarity, we have calculated activation energies required to generate these seven ions from $\mathbf{a}^{\bullet+}$, $\mathbf{b}^{\bullet+}$, and relevant isomers with the assumption that the dissociations do not involve reverse activation energies. Fragment optimized geometries are available upon request to the authors.

Formation of *m/z* 54 Ions. Formation of *m/z* 54 ions from $\mathbf{a}^{\bullet+}$ and $\mathbf{b}^{\bullet+}$ is the major fragmentation observed in high-energy CID spectra. It is also the most intense signal observed during low-energy CID experiments,[3] suggesting that generation of $[C_3,H_4,N]^+$ ions is the least energy-demanding dissociation. We report here the study of direct hydrogen loss, either from the methyl or from the methylene group of both $\mathbf{a}^{\bullet+}$ and $\mathbf{b}^{\bullet+}$, as

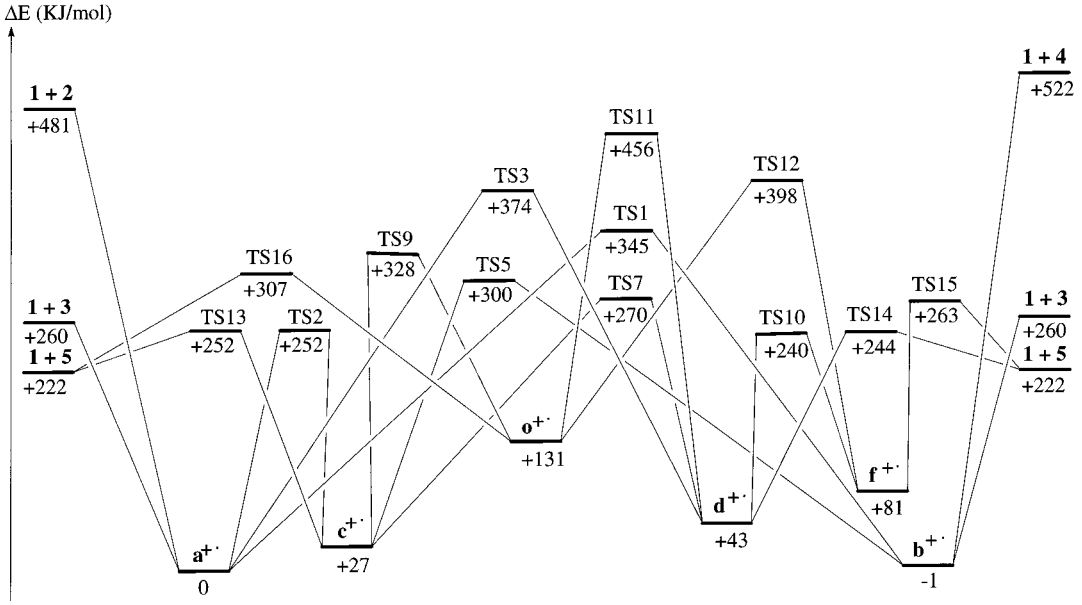

Figure 5. Stationary points on the potential energy surface associated with the formation of *m*/*z* 54 ions from $\mathbf{a}^{\bullet+}$, $\mathbf{b}^{\bullet+}$, and related isomers.

well as C−H bond cleavage after preliminary isomerization. UQCISD(T)/6-31G(d,p) total energies, and relative energies by reference to $\mathbf{a}^{\bullet+}$, of the fragments and related transition-state structures are given in Table 4. The overall fragmentation pattern is presented in Figure 5.

Direct loss of a hydrogen atom from the methyl group of $\mathbf{a}^{\bullet+}$ and $\mathbf{b}^{\bullet+}$ leads to fragments **1** + **3** (see Table 4). The cation $[CH_2{=}C{=}N{=}CH_2]^+$ has a linear cumulenic structure, and its calculated heat of formation is about 1000 kJ/mol by reference to $\Delta_fH°_{298}([CH_2{=}CH{-}C{\equiv}N{-}H]^+{=}\mathbf{6}) = 920$ kJ/mol.[7] Fragment **3** is much more stable than carbenic ions **2** and **4** (Table 4), which correspond to a loss of a hydrogen atom from the methylene group of $\mathbf{a}^{\bullet+}$ and $\mathbf{b}^{\bullet+}$, respectively. So, it turns out that C−H bond cleavage from the methyl group is favored. Attempts to locate the associated transition states for all these fragmentations failed; the different dissociations show in fact a monotonic increase of potential energy.

We have also considered the $[CH_2{=}CH{-}N{\equiv}CH]^+$ structure, **5**, which is more stable than **3**, and may be generated from $\mathbf{c}^{\bullet+}$, $\mathbf{d}^{\bullet+}$, $\mathbf{f}^{\bullet+}$, and $\mathbf{o}^{\bullet+}$. Calculation shows that these processes are characterized by small reverse energy barriers, especially for $\mathbf{c}^{\bullet+}$, $\mathbf{d}^{\bullet+}$, and $\mathbf{f}^{\bullet+}$ cations (+30, +22, and +41 kJ/mol, respectively; see Table 4). Since the energy barriers for $\mathbf{a}^{\bullet+} \rightarrow \mathbf{c}^{\bullet+}$, $\mathbf{b}^{\bullet+} \rightarrow \mathbf{c}^{\bullet+}$, and $\mathbf{c}^{\bullet+} \rightarrow \mathbf{d}^{\bullet+}$ isomerizations are in the same range of magnitude as those of the $\mathbf{a}^{\bullet+} \rightarrow \mathbf{1} + \mathbf{3}$ and $\mathbf{b}^{\bullet+} \rightarrow \mathbf{1} + \mathbf{3}$ fragmentations, it is clear that isomerization strongly competes with formation of $[CH_2{=}C{=}N{=}CH_2]^+$ from $\mathbf{a}^{\bullet+}$ and $\mathbf{b}^{\bullet+}$. Therefore, the peak at *m*/*z* 54 may correspond, at least, to two other structures, namely, **3** and **5**.

Formation of *m*/*z* 14, *m*/*z* 15, *m*/*z* 40, and *m*/*z* 41 Ions. Total and relative energies, by reference to $\mathbf{a}^{\bullet+}$ at the UQCISD(T)/6-31G(d,p)+ZPE level, of fragments corresponding to the formation of *m*/*z* 14, *m*/*z* 15, *m*/*z* 40, and *m*/*z* 41 ions are summarized in Table 4.

$CH_2^{\bullet+}$ may be produced by direct cleavage from $\mathbf{a}^{\bullet+}$, $\mathbf{b}^{\bullet+}$, $\mathbf{c}^{\bullet+}$, $\mathbf{f}^{\bullet+}$, or $\mathbf{m}^{\bullet+}$, together with CH_3CN, CH_3NC, CH_2NCH, CH_2NCH, CH_2CNH, respectively (Scheme 1).

If one considers the relative energies given in Table 4, it turns out that direct loss from $\mathbf{a}^{\bullet+}$ and $\mathbf{b}^{\bullet+}$ is the most favorable process. However, the most direct fragmentation, $\mathbf{a}^{\bullet+} \rightarrow \mathbf{7} + \mathbf{8}$, requires more energy than the $\mathbf{a}^{\bullet+} \rightarrow \mathbf{c}^{\bullet+} \rightarrow \mathbf{b}^{\bullet+}$ process, thus allowing a reversible isomerization prior to dissociation. So,

SCHEME 1

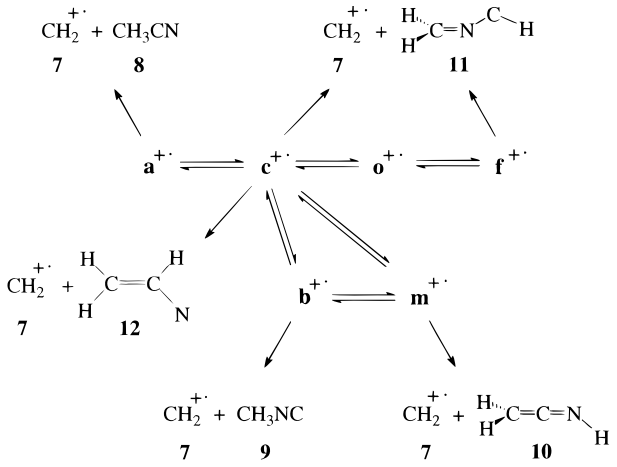

the preferable neutral fragment is likely to be acetonitrile, since the calculated energy difference between CH_3CN and CH_3NC is 106 kJ/mol. Note that this latter value is in good agreement with the difference of their experimental heats of formation (99 kJ/mol, with $\Delta_fH°_{298}(CH_3CN) = 74$ kJ/mol[7] and $\Delta_fH°_{298}(CH_3NC) = 173$ kJ/mol [7]). Moreover, from the values quoted in Table 4, acetonitrile and methyl isocyanide appear more stable than their respective tautomeric forms, CH_2CNH and CH_2NCH, by at least 130 kJ/mol. Finally, formation of $[CH_2]^{\bullet+}$ from $\mathbf{c}^{\bullet+}$ could also lead to the vinyl−nitrene species CH_2CHN. No optimized structure was found for this molecule in its closed-shell single state, and the optimization converged to CH_2CNH, via a 1,3-H shift. In the triplet ground state, the dissociation energy amounts to 730 kJ/mol.

The products of methyl cation formation and methyl radical loss have also been investigated.

The ions $\mathbf{a}^{\bullet+}$, $\mathbf{b}^{\bullet+}$, and $\mathbf{d}^{\bullet+}$ may lead directly to $[CH_3]^+$ ions (*m*/*z* 15). The associated radicals are $[CH_2NC]^{\bullet}$, $[CH_2CN]^{\bullet}$, and $[HCNH]^{\bullet}$, respectively. The latter one, which has formally carbenic and radical sites, does not correspond to a minimum but rather to a saddle point with one imaginary frequency. Calculations also demonstrate a higher stability of the cyano form with respect to its isocyano isomer. Thus, $\mathbf{a}^{\bullet+} \rightarrow \mathbf{13} + \mathbf{14}$ is less favorable than $\mathbf{b}^{\bullet+} \rightarrow \mathbf{13} + \mathbf{15}$. Moreover, both

SCHEME 2

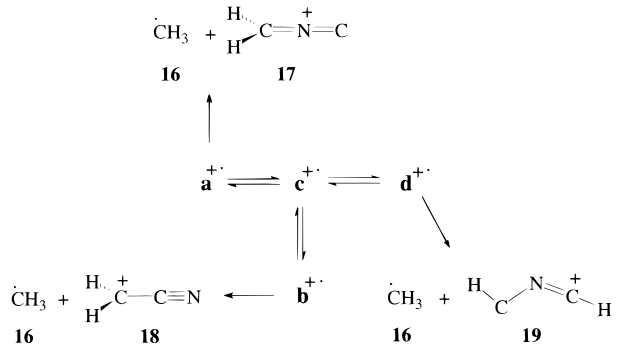

dissociations need more activation energy than is necessary for the interconversion between $\mathbf{a}^{\bullet+}$ and $\mathbf{b}^{\bullet+}$. Therefore, $[CH_3]^+$ ions should be preferably formed together with the $[CH_2CN]^\bullet$ radical in going from both $\mathbf{a}^{\bullet+}$ and $\mathbf{b}^{\bullet+}$.

Combination of values given in Tables 1 and 4 allow the following energies of fragmentation to be estimated:

$$CH_3CH_2NC^{\bullet+} \rightarrow CH_3^+ + CH_2NC^\bullet \qquad \Delta E = 229 \text{ kJ/mol}$$

$$CH_3CH_2CN^{\bullet+} \rightarrow CH_3^+ + CH_2CN^\bullet \qquad \Delta E = 150 \text{ kJ/mol}$$

$$CH_3CH_2NC^{\bullet+} \rightarrow {}^\bullet CH_3 + CH_2NC^+ \qquad \Delta E = 174 \text{ kJ/mol}$$

$$CH_3CH_2CN^{\bullet+} \rightarrow {}^\bullet CH_3 + CH_2CN^+ \qquad \Delta E = 179 \text{ kJ/mol}$$

These estimates, combined with $\Delta_f H°_{298}(CH_3CH_2CN^{\bullet+}) = 1194$ kJ/mol,[7] $\Delta_f H°_{298}(CH_3CH_2NC^{\bullet+}) = 1222$ kJ/mol,[7] $\Delta_f H°_{298}(CH_3^+) = 1093$ kJ/mol,[7] and $\Delta_f H°_{298}({}^\bullet CH_3) = 146$ kJ/mol,[7] lead us to propose $\Delta_f H°_{298}(CH_2CN^\bullet) = 251$ kJ/mol, in good agreement with the tabulated value (254 ± 10 kJ/mol[7]), and $\Delta_f H°_{298}(CH_2NC^\bullet) = 358$ kJ/mol.

The *m*/*z* 40 ions may correspond to $[CH_2NC]^+$, $[CH_2CN]^+$, and $[HCNH]^+$ (Scheme 2). Unlike neutral forms, the $[HCNCH]^+$ cation corresponds to a local minimum but, as expected, is less stable than cations **17** and **18**. The cyano form is slightly more stable than the isocyano form. In this context, direct losses of the methyl radical from $\mathbf{a}^{\bullet+}$ and $\mathbf{b}^{\bullet+}$ are the most favorable fragmentation routes, but they compete unfavorably with the various isomerization channels. Therefore, structural modifications before dissociation are allowed. Combination of the aforementioned energies of fragmentation with $\Delta_f H°_{298}(\mathbf{h}^{\bullet+})$, $\Delta_f H°_{298}(\mathbf{i}^{\bullet+})$, and $\Delta_f H°_{298}(CH_3^+)$ leads to $\Delta_f H°_{298}(CH_2CN^+) = 1227$ kJ/mol, which matches fairly with the tabulated value (1214 kJ/mol[7]), and to $\Delta_f H°_{298}(CH_2NC^+) = 1250$ kJ/mol.

Scheme 3 presents the possible fragmentations giving rise to *m*/*z* 41 ions directly from $\mathbf{a}^{\bullet+}$, $\mathbf{b}^{\bullet+}$, and related isomers. Results given in Table 4 indicate that ionized acetonitrile and methyl isocyanide are less stable than their tautomeric forms, $[CH_2CNH]^{\bullet+}$ and $[CH_2CNH]^{\bullet+}$, by 299 and 183 kJ/mol, respectively. Ionization energy measurements made by Leeck et al.[11] lead to the same conclusion. But surprisingly, by use of the heats of formations derived from these experiments, the difference of stability is not that important, namely, 155 kJ/mol for $[CH_2CNH]^{\bullet+}/[CH_3CN]^{\bullet+}$ and 71 kJ/mol for $[CH_2NCH]^{\bullet+}/[CH_3NC]^{\bullet+}$. In conclusion, *m*/*z* 41 ions observed in high-energy CID spectra are likely to correspond essentially to $[CH_2CNH]^{\bullet+}$ or $[CH_2NCH]^{\bullet+}$ via preliminary isomerization of $\mathbf{a}^{\bullet+}$ and $\mathbf{b}^{\bullet+}$.

Generation of *m*/*z* 27 and *m*/*z* 28 Ions. The two last dissociations studied correspond to generation of *m*/*z* 27 and *m*/*z* 28 ions. UQCISD(T)/6-31G(d,p) relative energies, corrected

SCHEME 3

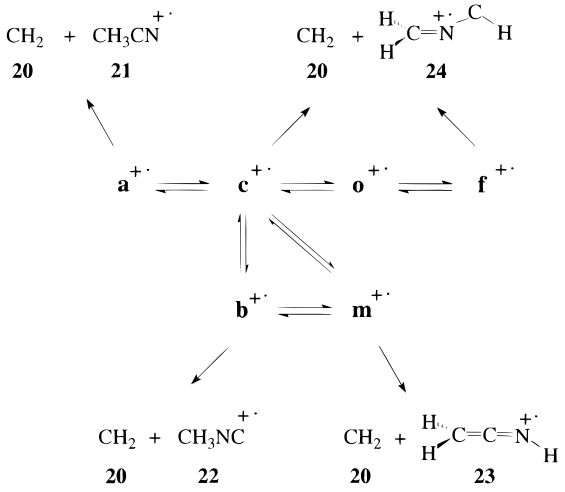

from the ZPE contributions, of the corresponding fragments are listed in Table 5. As shown in Scheme 4, *m*/*z* 27 ions may be either $[C_2H_3]^+$ or $[HCN]^{\bullet+}$ ions via homolytic and/or heterolytic fragmentations, respectively, which are both energy-demanding.

Owing to the different precursors employed, molecular ions of hydrogen cyanide are formed together with either ethylene, **27**, or ethylidene, **25**. The latter species, a carbenic structure in which the methyl group can freely rotate, has a triplet ground state lying 283 kJ/mol above ethylene. Therefore, $[HCN]^{\bullet+}$ should preferably be formed together with ethylene. However, results given in Table 5 clearly indicate that generation of $[HCN]^{\bullet+}$ is less favorable than formation of $[C_2H_3]^+$ ions. This latter entity has a bridged structure, which is more stable than the classic one (C_{2v} symmetry) by 7 kJ/mol at the level of theory utilized here. Calculations made by Herbst et al.,[17] concerning the study of the $[C_2H_2]^{\bullet+} + H_2$ association reaction, lead to the same conclusion. Note also the greater stability of **30**, in comparison with **29** (see Table 5).

Generation of *m*/*z* 28 and *m*/*z* 27 ions involves the cleavage of the same bonds for each of the four processes (Scheme 5). But when the relative energies given in Table 5 are inspected, these processes appear to be much more easier to achieve when leading to *m*/*z* 28 ions. Moreover, two of them ($\mathbf{f}^{\bullet+} \rightarrow \mathbf{32} + \mathbf{33}$ and $\mathbf{o}^{\bullet+} \rightarrow \mathbf{34} + \mathbf{35}$), which are formally single-bond elongations, are in the same energy range as formation of $[C_3H_4N]^+$ ions. This is in agreement with the fact that peaks at mass-to-charge ratios 28 and 54 are the most intense in high-energy CID spectra of $\mathbf{a}^{\bullet+}$ and $\mathbf{b}^{\bullet+}$. Moreover, since $\mathbf{a}^{\bullet+}$ and $\mathbf{b}^{\bullet+}$ cannot give directly stable *m*/*z* 28 ions, this intense peak is indicative of an isomerization prior to dissociation and should correspond to protonated hydrogen cyanide and mainly to ionized ethylene. Concerning the latter species, the most stable geometry is planar at the UHF/6-31G(d,p) level, whereas a torsional angle of 4° is found at the UMP2/6-31G(d,p) level (the experimental value being around 25°[18]). Ionized ethylidene has a geometry similar to that of its neutral triplet counterpart, and the difference of energy with $[CH_2{=}CH_2]^{\bullet+}$ is reduced to 128 kJ/mol by comparison with the neutrals. Moreover, protonated hydrogen cyanide, unlike the $[HCNH]^\bullet$ radical, is found to be linear. Finally, calculation shows that the very unstable species $[CH_2N]^+$ is probably not formed during the high-energy CID experiments.

In summary, this study provides an explanation for the similarity in the high-energy CID spectra of $\mathbf{a}^{\bullet+}$ and $\mathbf{b}^{\bullet+}$. Indeed, calculations suggest that these ions may isomerize prior to dissociation for several reasons: (a) the isomerization requires

TABLE 5: Calculated Total Energies (hartree)) and Relative and Zero-Point Energies (kJ/mol) of Fragments Corresponding to Formation of *m/z* 27 and *m/z* 28 Ions

structures	corresponding fragment number	(u)QCISD(T)/6-31G(d,p)[a]	ZPE[b]	ΔE[c]
	Formation of *m/z* 27			
$CH_3CH + HCN^{\bullet+}$	**25** + **26**	−170.930 368	155	+841
$CH_2{=}CH_2 + HCN^{\bullet+}$	**27** + **26**	−171.042 054	166	+558
$C_2H_3^+$ (bridged) + $HCNH^{\bullet}$	**28** + **29**	−171.080 886	150	+440
$C_2H_3^+$ (bridged) + $CH_2N^{\bullet}$	**28** + **30**	−171.098 543	149	+397
	Formation of *m/z* 28			
$CH_3CH^{\bullet+} + HCN$	**31** + **32**	−171.093 223	158	+347
$CH_2{=}CH_2^{\bullet+} + HCN$	**33** + **32**	−171.171 593	167	+219
$^{\cdot}CH_2CH + HCNH^+$	**34** + **35**	−171.144 656	162	+285
$^{\cdot}CH_2CH + CH_2N^+$	**34** + **36**	−170.820 750	150	+1123

[a] Based on UMP2/6-31G(d,p) optimized geometries. [b] Zero-point energies based on UHF/6-31G(d,p) harmonic vibrational wavenumbers and scaled by 0.9. [c] Relatives energies including UQCISD(T)/6-31G(d,p) values and ZPE corrections, by reference to $\mathbf{a}^{\bullet+}$.

SCHEME 4

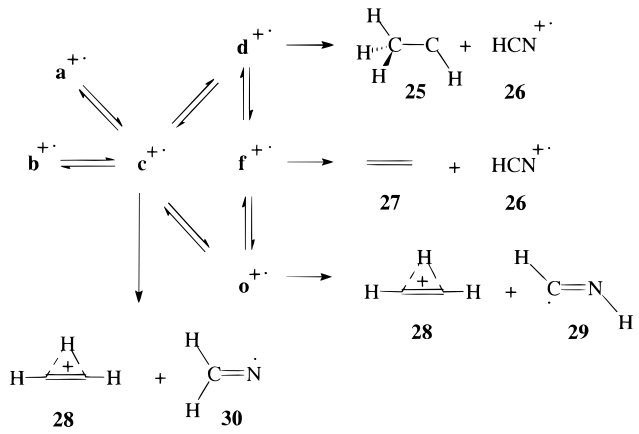

SCHEME 5

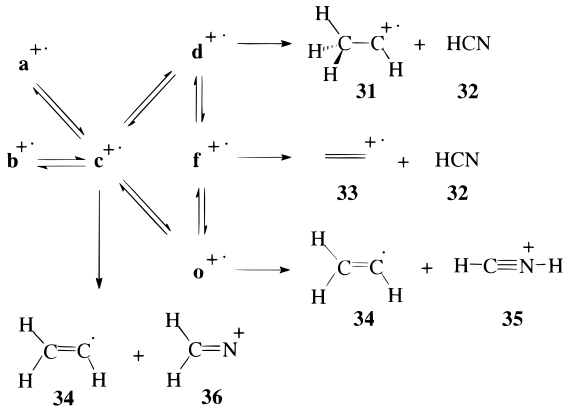

$\mathbf{a}^{\bullet+}$ and $\mathbf{b}^{\bullet+}$ to have about 300 kJ/mol of internal energy, an amount very likely to be transferred to ionic species during high-energy CID experiments; (b) fragmentations leading to *m/z* 14, 15, 27, 40, and 41 cations need more activation energy than isomerization processes in such a way that structural modifications of parent ions may occur before generation of these ions; (c) direct losses of a hydrogen atom from $\mathbf{a}^{\bullet+}$ and $\mathbf{b}^{\bullet+}$ are similar in terms of demanding energy and compete strongly with production of $[CH_2{=}CH{-}N{\equiv}CH]^+$ species from $\mathbf{c}^{\bullet+}$, $\mathbf{d}^{\bullet+}$, and $\mathbf{f}^{\bullet+}$; (d) easy intense *m/z* 28 ions suggest a previous isomerization of $\mathbf{a}^{\bullet+}$ and $\mathbf{b}^{\bullet+}$. Finally, the most favorable dissociations calculated (leading to *m/z* 28 and 54 ions) correspond to the most intense peaks of the CID spectra.

Conclusion

Ab initio molecular orbital calculations show that acetonitrile *N*-methylide $[CH_3{-}C{\equiv}N{-}CH_2]^{\bullet+}$, $\mathbf{a}^{\bullet+}$, and *N*-methylketenimine $[CH_3{-}N{\equiv}C{-}CH_2]^{\bullet+}$, $\mathbf{b}^{\bullet+}$, are the most stable species among the 15 isomers considered. Use of ionized propionitrile and ethylisocyanide as standards allow us to propose a heat of formation of 970 kJ/mol for both species. This study of isomerization processes involving 1,*n*-H shifts revealed that $\mathbf{a}^{\bullet+}$ and $\mathbf{b}^{\bullet+}$ are located in deep energy wells and therefore constitute a distinct species in the gas phase. It follows that $\mathbf{a}^{\bullet+}$ and $\mathbf{b}^{\bullet+}$ without large internal energy do not undergo interconvertion. This result is in excellent agreement with the observed difference of reactivity of $\mathbf{a}^{\bullet+}$ and $\mathbf{b}^{\bullet+}$ toward dimethyl disulfide, since these reactions were preceded by a deceleration of ions and thus implied collisionally unexcited species.[3]

This study also confirms that isomerization of $\mathbf{a}^{\bullet+}$ and $\mathbf{b}^{\bullet+}$ probably takes place prior to dissociation during high-energy CID experiments, as expected in view of their very similar CID spectra. The 300 kJ/mol of internal energy necessary for each of the ions $\mathbf{a}^{\bullet+}$ and $\mathbf{b}^{\bullet+}$ to isomerize may easily be transferred during collisional activation. Examination of fragmentations leading to seven daughter ions supports this conclusion. Indeed, the energy theoretically required to produce *m/z* 14, 15, 27, 40, and 41 ions allows structural modifications of parent ions prior to dissociations. Moreover, $\mathbf{a}^{\bullet+}$ and $\mathbf{b}^{\bullet+}$ cannot directly give stable and intense *m/z* 28 ions, as observed in the spectra. Finally, formation of *m/z* 54 ions may indiscriminately involve either direct C−H bond cleavages from $\mathbf{a}^{\bullet+}$ and $\mathbf{b}^{\bullet+}$ or preliminary isomerization to $\mathbf{c}^{\bullet+}$, $\mathbf{d}^{\bullet+}$, and $\mathbf{f}^{\bullet+}$.

Acknowledgment. J.Y.S. and M.T.N. thank the FWO-Vlaanderen for financial support. P.G. thanks the "Fond National de la Recherche Scientifique" for a research fellowship.

References and Notes

(1) Drewello, T.; Heinrich, N.; Maas, W.; Nibbering, N. M. N.; Weiske, T.; Schwarz, H. *J. Am. Chem. Soc.* **1987**, *109*, 4810.

(2) Stirk, K.; Smith, R. L.; Orlowski, J. C.; Kenttämaa, H. I. *Rapid Commun. Mass Spectrom.* **1992**, *7*, 392.

(3) Gerbaux, P.; Flammang, R.; Nguyen, M. T.; Salpin, J. Y.; Bouchoux, G. *J. Phys. Chem. A* **1998**, *102*, 861.

(4) Frisch, M. J.; Trucks, G. W.; Schlegel, H. B.; Gill, P. M. W.; Johnson, B. G.; Robb, M. A.; Cheeseman, J. R.; Keith, T.; Petersson, G. A.; Montgomery, J. A.; Raghavachari, K.; Al-Laham, M. A.; Zakrzewski, V. G.; Ortiz, J. V.; Foresman, J. B.; Cioslowski, J.; Stefanov, B. B.; Nanayakkara, A.; Challacombe, M.; Peng, C. Y.; Ayala, P. Y.; Chen, W.; Wong, M. W.; Andres, J. L.; Replogle, E. S.; Gomperts, R.; Martin, R. L.; Fox, D. J.; Binkley, J. S.; Defrees, D. J.; Baker, J.; Stewart, J. P.; Head-Gordon, M.; Gonzalez, C.; Pople, J. A. *Gaussian 94*, revision E.2; Gaussian, Inc.: Pittsburgh, PA, 1995.

(5) Hall, H. K., Jr.; Baldt, J. H. *J. Am. Chem. Soc.* **1971**, *93*, 140.

(6) Mallard, W. G., Linstrom, P. J., Eds. *NIST Chemistry Webbook*; NIST Standard Reference Database 69; National Institute of Standards and Technology: Gaithersburg, MD, 1988 (http://webbook.nist.gov).

(7) Lias, S. G.; Bartmess, J. E.; Liebman, J. F.; Holmes, J. L.; Levin, R. D.; Mallard, W. G. *J. Phys. Chem. Ref. Data, Suppl. 1* **1988**, *17*.

(8) Chess, E. K.; Lapp, R. L.; Gross, M. L. *Org. Mass Spectrom.* **1982**, *17*, 475.
(9) Vayjooee, M. H. B.; Collister, J. L.; Pritchard, H. O. *Can. J. Chem.* **1977**, *55*, 2634.
(10) Kebarle, P.; Chowdhury, S. *Chem. Rev.* **1987**, *87*, 513.
(11) Leeck, D. T.; Kenttämaa, H. I. *Org. Mass Spectrom.* **1994**, *29*, 106.
(12) Bateman, R. H.; Brown, J.; Lefevere, M.; Flammang, R.; Van Haverbeke, Y. *Int. J. Mass Spectrom. Ion Processes* **1992**, *115*, 205.
(13) Bouchoux, G. *Mass Spectrom. Rev.* **1988**, *7*, 203.
(14) Rusli, R. D.; Schwarz, H. *Chem. Ber.* **1990**, *123*, 535.
(15) Schulz, R.; Schweig, A. *J. Electron Spectrosc. Relat. Phenom.* **1982**, *28*, 33.
(16) Bouchoux, G.; Salpin, J. Y.; Dutuit, O.; Palm, H.; Alcaraz, C. *Rapid Commun. Mass Spectrom.* **1995**, *9*, 1195.
(17) Herbst, E.; Yamashita, K. *J. Chem. Soc., Faraday Trans.* **1993**, *89*, 2175.
(18) (a) Merer, A. J.; Schoonveld, L. *Can. J. Phys.* **1969**, *47*, 1731. (b) Köppel, H.; Domcke, W.; Cederbaum, L. S.; Niessen, W. V. *J. Chem. Phys.* **1978**, *69*, 4252.